As originally published in the SMTA Proceedings.

Novel Lead-Free Solder Alloys Based on Sn-Ag-Cu-Sb with Enhanced Thermal and Electrical Reliability

Jie Geng, Ph.D. and Hongwen Zhang, Ph.D.
Indium Corporation
NY, USA
jgeng@indium.com; hzhang@indium.com

ABSTRACT
Since antimony (Sb) has the potential to improve the thermal fatigue resistance of solder joints in harsh conditions, the degree of such improvement in reliability depends on the alloying content of Sb, which is usually in the range of 1.5 to 9 wt.%. In this work, thermal performance of five Sn/3.2Ag/0.7Cu/xSb (x is in the range of 4.5 to 6.5 wt.%) alloys were compared to select the optimized Sb content. When shear testing was conducted at 25, 75, and 150°C, 90.6Sn/3.2Ag/0.7Cu/5.5Sb (Indalloy®276) showed the best performance at those temperatures. The shear test done for the 0805 chip resistors at intervals of TCT -40 to 125°C also confirmed that 5.5 wt.% of Sb promoted the best shear strength during thermal cycling. Thus, 90.6Sn/3.2Ag/0.7Cu/5.5Sb was identified and developed for testing in targeting high reliability with a wide service temperature capability. 90.6Sn/3.2Ag/0.7Cu/5.5Sb has a melting temperature range of 223–232°C and could be processed with traditional SAC305 reflow profiles. The thermal fatigue behavior was investigated under a thermal cycling profile of -40 to 125°C with 10 minutes dwell time at each extreme temperature. The thermal cycling tests were carried out using various components on daisy-chained test boards, such as CABGA192 and chip resistors (including 0805 and 0603). The degradation of solder alloys caused by thermal fatigue was evaluated with shear testing, in-situ electrical continuity monitoring, dye penetrant (Dye & Pry), and cross section investigation. Alloying with 5.5 wt% of Sb dramatically improved the thermal fatigue resistance compared to SAC305.

Key words: lead-free solder alloy, high reliability, thermal fatigue reliability, shear test

INTRODUCTION

With automotive electronics booming, especially those in electrical vehicles (EV), more sensors and power moderators are increasingly required for electrical vehicles and self-driving cars. Lead-free tin-silver-copper (SnAgCu), also known as SAC, has been a popular solder alloy choice for surface mount technology (SMT) assembly in the electronics industry. While SAC has served the electronics industry adequately well, its adoption for automotive applications has proved to be challenging for several reasons. Key amongst them is uncertainty in service temperature range capability [1-14]. There is no question that automotive applications demand high reliability. However, that high reliability is required not only under moderate temperatures, but also under high service temperature conditions. Only limited success has been achieved up to this point [13, 14]. In this work, a novel SnAgCu-based solder alloyed with Sb was developed and characterized for its reliability performance in chip resistors and CABGA192 under thermal cycling testing (TCT) of -40/125°C.

OPTIMIZATION of Sb CONTENT in Sn/3.2Ag/0.7Cu ALLOYS

Selection of Sb Contents Range

In the recent development of high-performance Pb-free solder alloys, Sb plays a key role in improving the thermal fatigue resistance of solder joints in harsh thermal cycling or thermal shock conditions. According to the binary Sn-Sb phase diagrams [15, 16], the solubility of Sb in Sn is approximately 0.5 wt. % at room temperature and about 1.5 wt. % at 125ºC. Due to the dissolution of Sb in Sn-based Pb-free solders, solid solution strengthening is expected in these alloys [17].

Apart from solid solution strengthening, alloying with Sb also has the potential to form various intermetallic phases (IMCs) with Sn resulting in the precipitation hardening [15]. In literature, 1.5 to 9.0 wt% of Sb has been reported. Those alloys showed different thermal fatigue resistance depending on the concentration of the alloyed Sb. The fine SnSb IMC particles nucleate and grow (cluster of different atoms in certain stoichiometric ratio) after solder solidification during reflow. These SnSb particles are reversely dissolved back into Sn matrix to form a solid solution with increasing temperature, and then precipitate out with the drop in temperature. A sufficient quantity of Sb is important to harden the solder alloy by providing both solid-solution and precipitation strengthening to the alloy [18]. When the amount of Sb is reduced below 3.0 wt%, fine SnSb particles are completely dissolved back into the Sn matrix to form a Sn-Sb solid solution when serving at 150°C and above; no SnSb fine particles remain to strengthen the alloy. Strengthening in alloys is associated with interrupting the dislocation movement. Both fine particles embedded in the alloy matrix and solute atoms in the solid solution act as obstacles to block the dislocation slide along the favorable lattice direction. At high temperatures (homologous temperature > 0.6), atomic diffusion plays an important role to assist the dislocation movement. For small obstacles like solute atoms, atomic diffusion can easily assist the dislocation to bypass or “climb over” the obstacles. For large obstacles like precipitates, more atomic diffusion steps are

needed to allow the dislocations to bypass or "climb over" the obstacles. Thus, precipitates are more valuable to maintain high-temperature strength through interrupting the dislocation movement.

Therefore, 4.5 wt% and above of Sb is expected to keep the alloys maintaining enough precipitate strengthening, even at 150°C and above. However, if the Sb addition exceeds 10 wt%, the solder alloys will have a liquidus temperature above 266°C, making it impossible to be reflowed by the conventional SAC305 process (the peak reflow temperature is usually below 245°C).

Therefore, the first goal of this work is to find the optimized Sb content to maintain a balanced strengthening effect. Five Sn/3.2Ag/0.7Cu/xSb alloys, A to E as shown in Table 1, were tested, and compared. These alloys contain Sb in the range of 4.5 to 6.5 wt.%.

Table 1. The compositions of Sb containing alloys (wt.%)

Alloy	Sn	Ag	Cu	Sb
A	91.6	3.2	0.7	4.5
B	91	3.2	0.7	5.1
C	89.3	3.2	0.7	5.5
D	90.2	3.2	0.7	5.9
E	89.6	3.2	0.7	6.5

Shear Test at Various Temperatures

Shear strength comparison tests were conducted at temperatures of 25°C, 75°C, and 150°C. All solder joints were reflowed with a peak temperature of 245°C. Test coupons were made using 3×3 mm Cu die on the 38×38 mm bare Cu substrate.

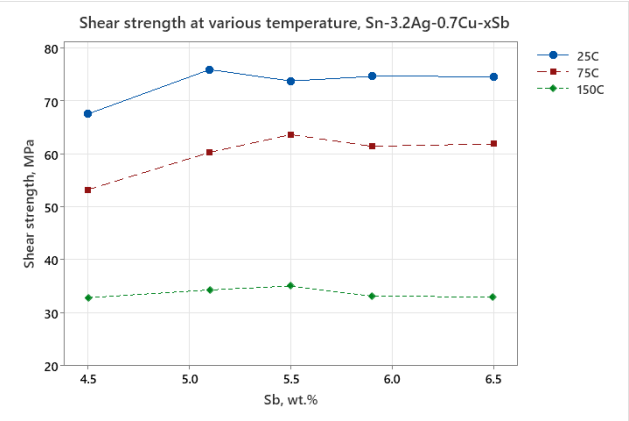

Figure 1. Shear strength of Sn/3.2Ag/0.7Cu/xSb alloys at 25°C, 75°C, and 150°C.

Figure 1 shows the shear strengths of all the alloys measured at various temperatures. Solder joints formed from solder alloys having greater than 5.0 wt.% to 6.0 wt.% of Sb (Alloys B, C, and D) outperformed solder joints formed from solder alloys having less than 5.0 wt.% and greater than 6.0 wt.% (Alloys A and E) in shear strength measurements. Shear strength performance was best for Alloy C (5.5 wt.% Sb). A solder joint formed from this alloy exhibited the highest shear strength at temperatures of 75°C and 150°C.

Shear Strength at Intervals of Thermal Cycling -40/125°C

The shear strength of the Sn/3.2Ag/0.7Cu/xSb alloys was also compared at different intervals during thermal cycling of -40/125°C with 10 minutes dwell time. The test vehicle was composed of surface mount resistors (SMR) 0805 on the PCB with an OSP surface finish, as shown in Figure 2.

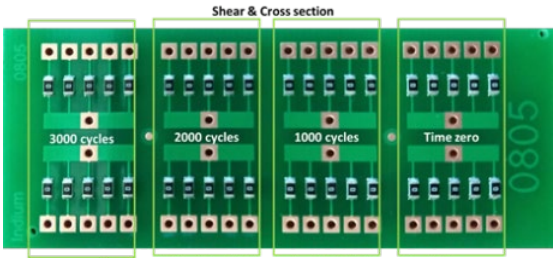

Figure 2. Test vehicle of SMR 0805 on PCB for shear test

First, the shear strength of the resistor was measured after reflow (time zero). Then, the boards were put into a thermal cycling (-40 to 125°C) chamber for 1000, 2000, and 4895 cycles. The measurements were plotted in Figure 3. After thermal cycling at -40 / 125°C, solder joints formed from solder alloys having greater than 5.0 wt.% to 6.0 wt.% of Sb (Alloys B, C, and D) maintained their shear strength better than those formed from solder alloys having less than 5.0 wt.% and greater than 6.0 wt.% (Alloys A and E).

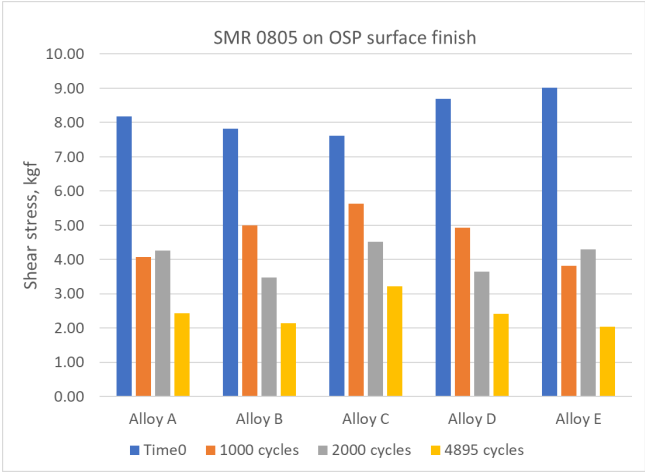

Figure 3. The shear strength of Sn/3.2Ag/0.7Cu/xSb alloys after 1000, 2000, and 4895 cycles of thermal cycling at -40 / 125°C.

Referring to both Figures 1 and 3, Alloy C shows the best performance over the others. Therefore, 5.5 wt.% of Sb is the optimized Sb content to promote better high-temperature performance. The alloy consisting of 90.6Sn/3.2Ag/0.7Cu/5.5Sb (IND276) was selected as the high-reliability and high-performance Pb-free solder alloy for further thermal fatigue reliability tests.

THERMAL RELIABILITY OF 90.6Sn/3.2Ag/0.7Cu/5.5Sb (IND276)

Thermal Cycling Test -40/125°C: Chip Resistor

As seen in Figure 2, a daisy-chained resistor board—having both OSP and ImSn surface finishes on the pads—was designed to test the thermal reliability of solder alloys. The board was designed with two different sized chip resistors, 0805 and 0603. The pad was solder-mask-defined. The shear strength and the cross section of the solder joint were examined at various intervals during the thermal cycle test (TCT) at -40 to 125°C. The dwell time of the thermal cycling test was 10 minutes. SAC305 (Sn/3.0Ag/0.5Cu) was used as the control for comparison.

Shear testing was done to check the bonding strength at intervals of 0, 1500, and 3000 cycles under TCT (-40/125°C). The data was plotted as shown in Figure 4. For all types of chip resistors, SAC305 showed more than 50% of shear strength drop after 3000 cycles compared to time zero (before TCT). The shear strength of joints with IND276 held up well. The shear strength of SMR0805 after 3000 cycles had almost no change compared to 1500 cycles, i.e., the microstructure of the joints was quite stable between 1500 and 3000 cycles.

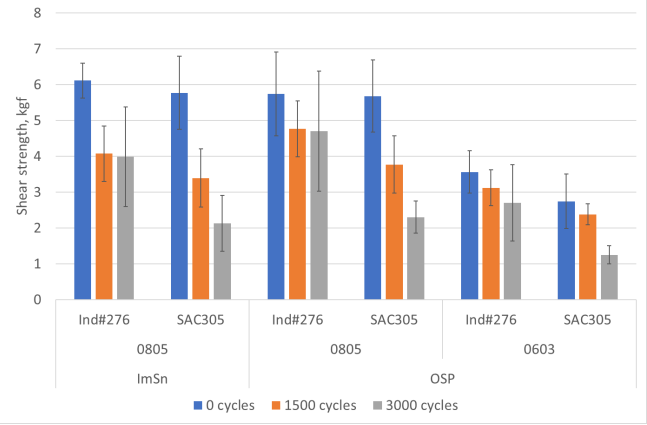

Figure 4. Shear strength of SMR0603 and SMR0805 resistors for SAC305 and IND276 alloys at 0, 1500, and 3000 cycles under TCT (-40/125°C).

After a certain number of thermal cycles, cross sections of the chip resistors were examined to check the formation and propagation of fatigue cracks. Figures 5–7 show the cross-sectional optical micrographs of SMR0805 and SMR0603 on the OSP and ImSn surface finishes. It is obvious from Figure 5 that the joints of both SAC305 and IND276 on the OSP surface finish were intact in first 1000 cycles at TCT -40/125°C. SAC305 exhibited cracks after 1500 cycles while IND276 had no cracks. For the joints with IND276, a crack was developed after 2500 cycles and only noticeable after 3000 cycles. The joints with SAC305 exhibited a fully propagated crack under the termination after 1500 cycles.

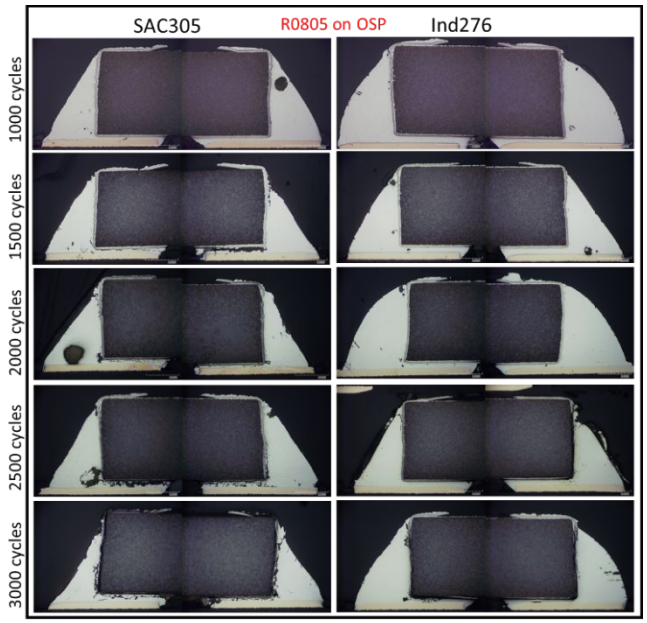

Figure 5. Cross-sectional optical micrographs of SMR0805 on the OSP surface finish after 1000, 1500, 2000, 2500, and 3000 cycles under TCT -40/125°C.

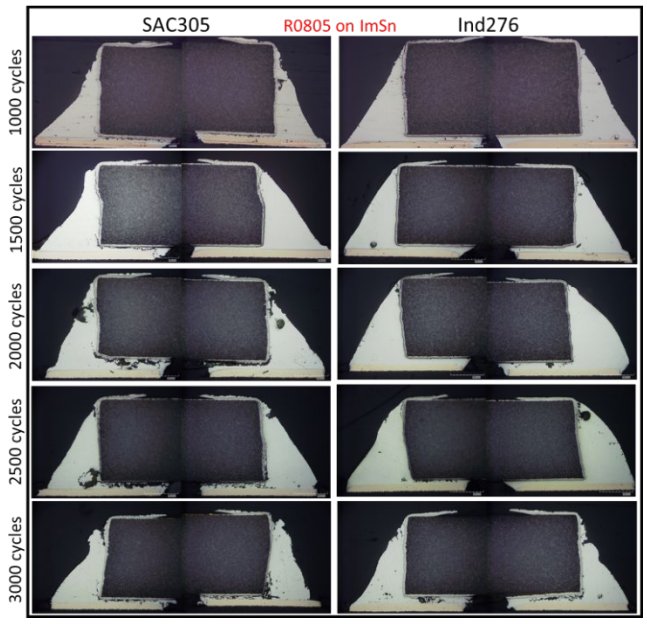

Figure 6. Cross-sectional optical micrographs of SMR0805 on the ImSn surface finish after 1000, 1500, 2000, 2500, and 3000 cycles under TCT -40/125°C.

The crack propagation for the joints on the ImSn surface finish formed earlier than those on the OSP, as shown in Figure 6. SAC305 exhibited cracks even after 1000 cycles while it was intact on the OSP surface finish (Figure 5). IND276 started to show cracks after 2500 cycles on the ImSn surface finish while the crack was not noticeable after 2500 cycles on the OSP surface finish (Figure 5). After 2000 cycles, the crack propagated fully under the termination of the resistors.

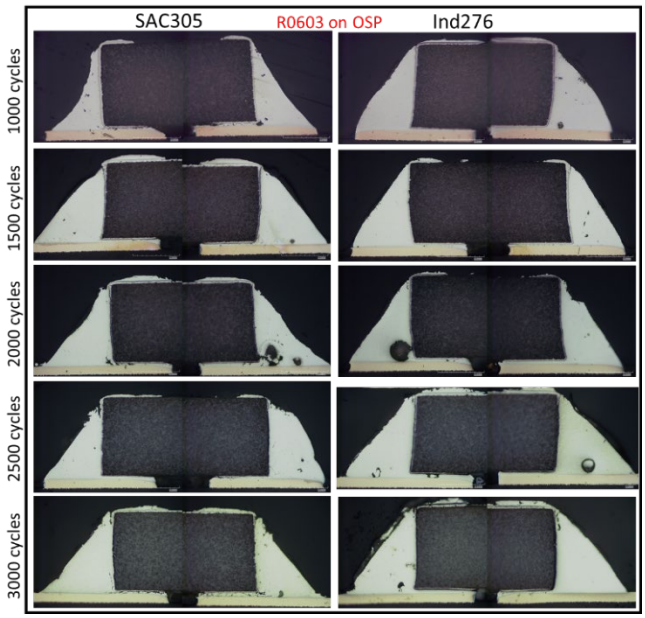

Figure 7. Cross-sectional optical micrographs of SMR0603 on the OSP surface finish after 1000, 1500, 2000, 2500, and 3000 cycles under TCT -40/125°C.

As shown in Figure 7, the cracks in the SMR0603 resistors on the OSP surface finish was noticeable after 2500 cycles for SAC305. No cracks were noticeable in the joints of IND276 even after 3000 cycles.

As seen in Figures 5–7, SAC305 showed more cracks than IND276 at each interval under TCT -40/125°C. Furthermore, the crack formed earlier in SAC305 than in IND276. The crack propagation was quantified in resistors of SAC305 and IND276 after 2000 and 3000 cycles. Figure 8 shows the calculated crack ratio at various intervals. For the SMR0805, the crack ratio in SAC305 after 3000 cycles was more than 70% on both the ImSn and OPS surface finishes. The crack ratio after 3000 cycles in the resistors of IND276 was only 23% on the ImSn surface finish and 43% on the OSP surface finish. IND276 showed much improved crack resistance compared to SAC305.

The observations from cross sections of the resistors agree with the shear strength data as shown in Figure 4. The presence of the severe cracking results in significant shear strength drops in SAC305 after 3000 cycles.

Figure 9 shows the SEM images of the SMR0805 resistor on the ImSn surface finish for both SAC305 and IND276 at 0, 2000, and 3000 cycles. After 2000 cycles, no crack was observed in the joint of IND276 compared to the heavily cracked SAC305. The cracks propagated in the bulk solder joints for both SAC305 and IND276.

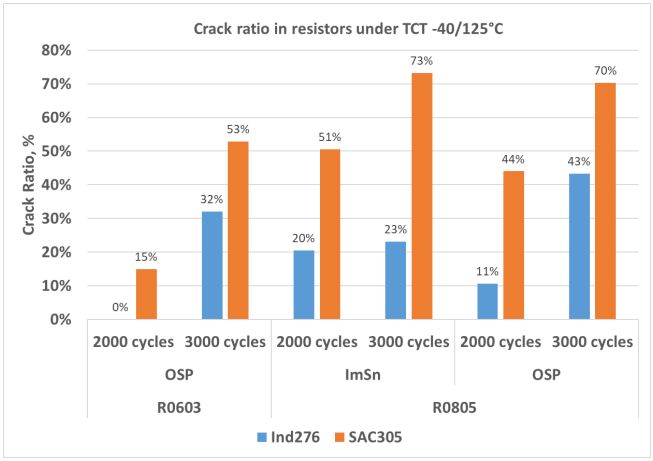

Figure 8. The crack ratio in resistors of SAC305 and IND276 after 2000 and 3000 cycles under TCT -40/125°C.

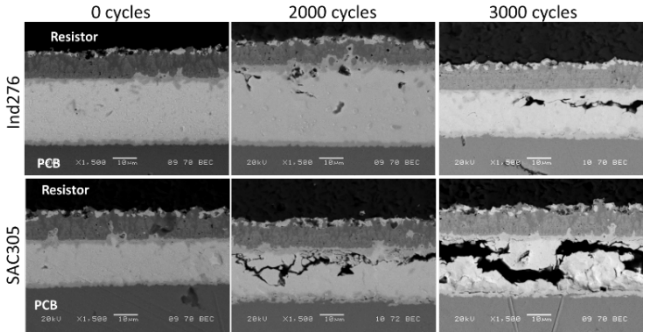

Figure 9. Backscattered electron SEM images of the cross sections of SMR0805 resistors on the ImSn surface finish after 0, 2000, and 3000 cycles under TCT -40/125°C.

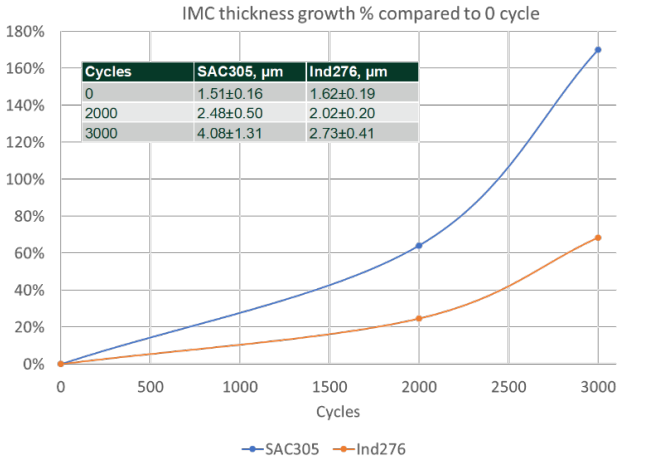

Cycles	SAC305, µm	Ind276, µm
0	1.51±0.16	1.62±0.19
2000	2.48±0.50	2.02±0.20
3000	4.08±1.31	2.73±0.41

Figure 10. The IMC layer thickness growth rate (compared to zero cycle) in SMR0805 resistors of SAC305 and IND276 at 2000 and 3000 cycles under TCT -40/125°C.

In the SEM images in Figure 9, the IMC layer thickness at the PCB side were measured at 0, 2000, and 3000 cycles under TCT -40/125°C. Figure 10 shows the IMC thickness growth rate of SMR0805 resistors in the joints of SAC305 and IND276. The growth rate was calculated based on IMC

thickness at 0 cycles. Before the thermal cycling test, the IMC layer thickness in both SAC305 and IND276 was very close—1.51 and 1.62µm respectively. After 2000 cycles, the IMC layer in SAC305 grew more than 60% to 2.48µm. At 2000 cycles, the IMC growth rate in SAC305 is nearly tripled than that in IND276. Furthermore, between 2000 and 3000 cycles, the IMC layer grew significantly in SAC305. The thickness was 170% more than its value at 0 cycles while the IMC layer thickness grew only 70% after 3000 cycles in IND276.

The data shown in Figure 10 is consistent with the studies by Li, et al. who reported that Sb slows the growth rate of the Cu_6Sn_5 intermetallic compound (IMC) layers at the attachment interfaces [19, 20]. Fast interfacial IMC growth on Cu surfaces tends to produce irregular and non-uniform IMC layers. This can lead to reduced mechanical reliability by inducing fractures at IMC interfaces or through the IMC in drop shock loading [21]. The observations shown in Figure 9 indicate that alloying with Sb may improve thermal fatigue performance through slowing the IMC growth apart from the solid solution strengthening and precipitation hardening mechanisms.

Thermal Cycling Test -40/125°C: CABGA192

The printed circuit board (PCB) test vehicle was 1.54 mm-thick with a 4-layer construction and with 12 sites for the CABGA192, as shown in Figure 11. Boards were fabricated with two different surface finishes, OSP and ImSn. The size of the CABGA192 is 14×14 mm. Ball pitch is 0.8mm and ball diameter is 0.46mm. In this study, the cross section of the CABGA was done with the first row as shown in Figure 11. From left to right, the balls were marked as B01 to B16.

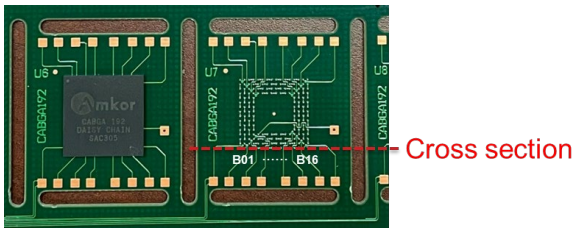

Figure 11. The fully populated CABGA192 PCB test board used in this study and the location where the cross sections were examined.

TCT -40/125°C was performed for CABGA192 test boards with OSP and ImSn surface finishes and the test was stopped after 5800 cycles. Each alloy had a sample size of 12 BGAs for each type of surface finish. The resistance of the BGAs was monitored using a data logger and the failure was identified by electrical opens.

The Weibull analysis with right-censored data for the CABGA192 on the OSP and ImSn surface finishes is plotted in Figure 12. The characteristic life for SAC305 on ImSn is 4741 cycles, while that for IND276 is 5555 cycles. For the OSP surface finish, IND276 performed similarly to the ImSn surface finish. SAC305 showed improved characteristic life on the OSP surface finish, which increased from 4741 cycles on ImSn to 5494 cycles on OSP.

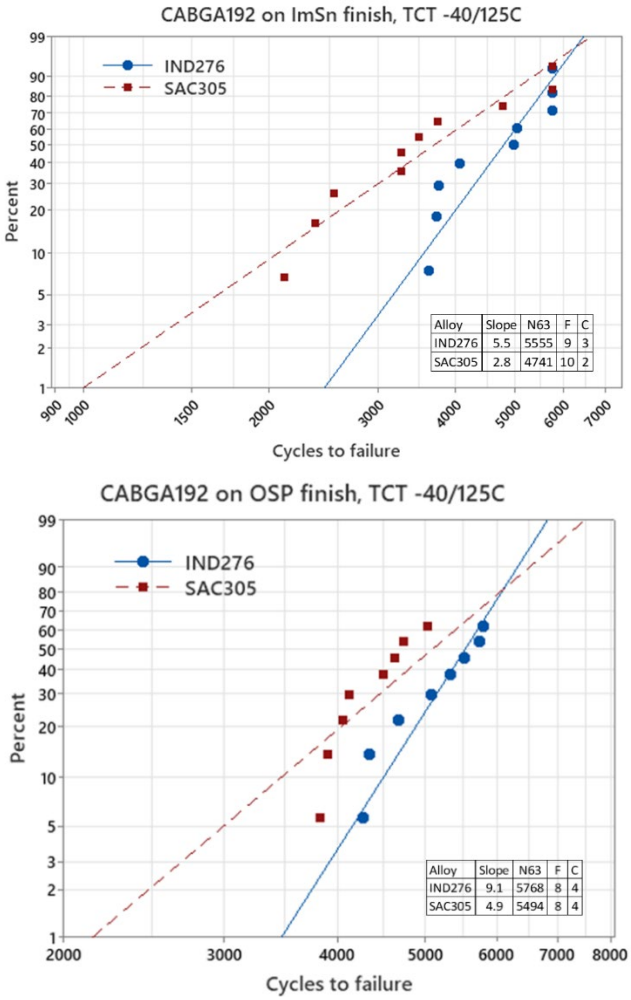

Figure 12. Right-censored Weibull plots for SAC305 and IND276 tested with the CABGA192 on ImSn and OSP surface finishes under TCT -40/125°C.

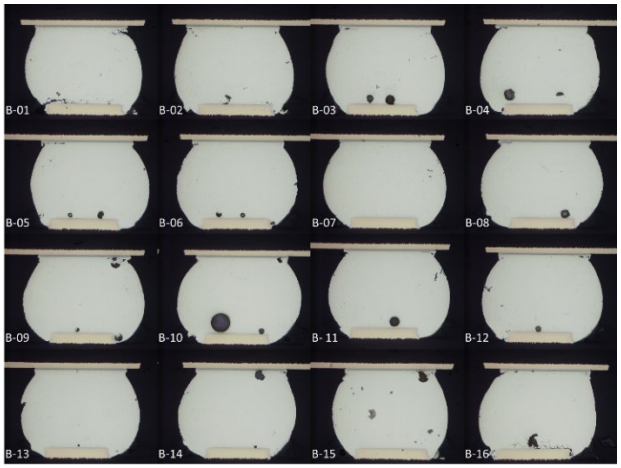

Figure 13. The cross section of CABGA192 of SAC305 on the ImSn surface finish after 3000 cycles under -40/125°C.

Apart from the in-situ resistance monitoring for Weibull analysis, another set of CABGA192 test boards were used for cross section analysis. The cross sections of the CABGA192 were done at 1000, 1600, 2000, and 3000 cycles to compare the crack propagation in the joints of SAC305 and IND276. As shown in Figure 11, the cross section was done with the outmost row of the ball grid array. The balls were marked as B01 to B16 from left to right. The B01 and B16 are the corner joints. Figure 13 shows a typical cross section optical image from one BGA192 chip. In Figure 13, it is the SAC305 on the ImSn surface finish after 3000 cycles. The corner joints B01 and B16 showed more cracks than other joints.

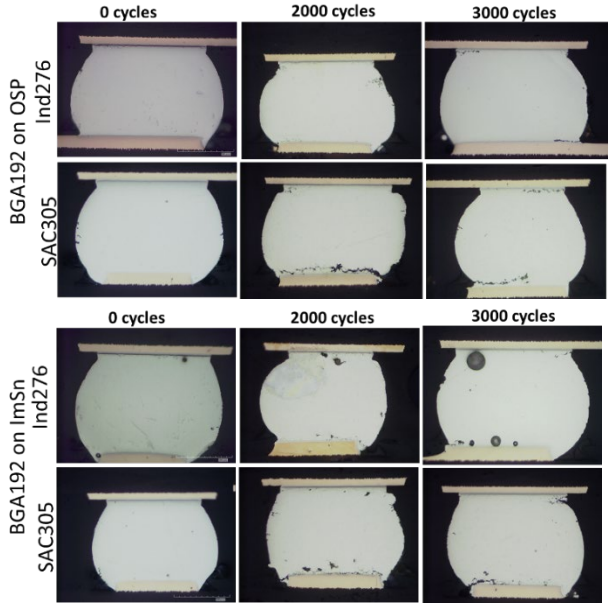

Figure 14. Comparison of the cross sections of corner joints from BGA192 of SAC305 and IND276 at 0, 2000, and 3000 cycles under -40/125°C.

Figure 14 shows the comparison of BGA192 joints of SAC305 and IND272 at 0, 2000, and 3000 cycles. The images were chosen from the corner joints. It is obvious that on both ImSn and OSP surface finishes, SAC305 exhibited more cracks than IND276 at specific intervals of TCT -40/125°C. At 2000 cycles, SAC305 showed several cracks at the PCB side but IND276 did not.

The crack ratios for each joint (BGA balls) were calculated from the cross section optical images at 1000, 1600, and 3000 cycles. The measurements were taken at both the component (BGA192) side and the PCB side. The data was plotted in Figure 15, where each row was16 balls from left to right and the number shown in each individual square was the crack ratio for that specific joint/ball. For each interval, the plot used a scaled color scheme for the crack ratio. At 1000 cycles, cracks were very limited in both SAC305 and IND276. No crack was observed in IND276. SAC305 had cracks in the corner joints only at the PCB side. The crack initiation and propagation in IND276 was very limited up to 1600 cycles. The corner joints at the PCB side in SAC305 exhibited more than a 50% crack ratio after 1600 cycles. After 3000 cycles, both SAC305 and IND276 alloys showed cracks not only at the PCB side but also at the component side. SAC305 had a higher crack ratio than IND276 and one of joints was fully open.

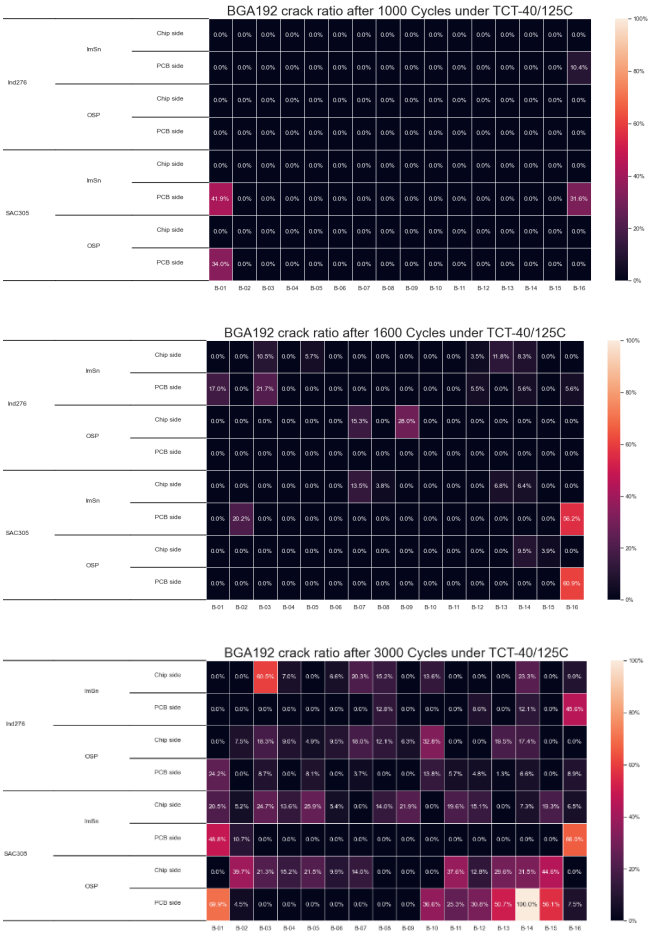

Figure 15. The crack ratio of each joint/ball at both the component side and PCB side in SAC305 and IND276 at 1000, 1600, and 3000 cycles under TCT -40/125°C.

After stopping at 5800 cycles under TCT -40/125°C, Dye & Pry testing was conducted for the BGA192 chips. Figure 16 shows a typical optical image taken from SAC305 on the ImSn surface finish (PCB side). Based on the dyed area percentage, the joints were categorized into five groups: 0 for no cracks; 1 for less than a 25% crack area; 2 for a crack area % between 25% and 50%; 3 for a crack area % between 50% and 75%; and 4 for a crack area % between 75% and 100%. The statistics of the crack area % categories were plotted in Figure 17. For the OSP surface finish, 39% (out of 192) joints/balls had a cracked area of 75% in SAC305 after 5800 cycles while it was only 11% in IND276. Meanwhile, IND276 had 53% of the joints without cracks compared to 39% in SAC305. On the ImSn surface finish, SAC305 performed better than itself on the OSP surface finish, where only 11% of the joints had more than 75% of cracked areas.

Figure 16. Dye & Pry optical image from SAC305 BGA192 chips on the ImSn surface finish after 5800 cycles under TCT -40/125°C and the calculated crack area % for each joint/ball.

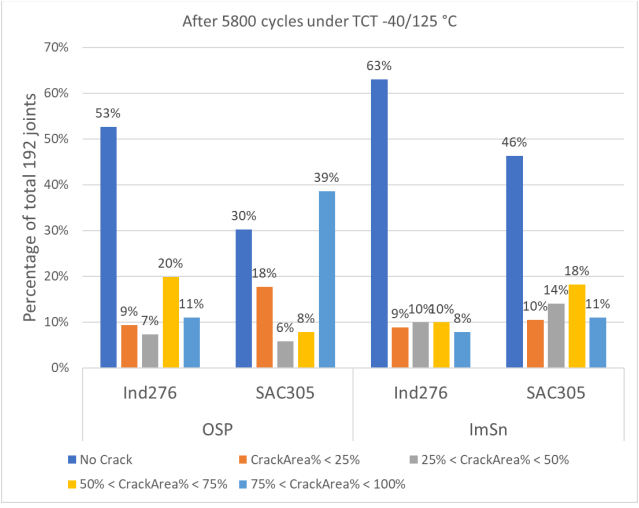

Figure 17. Statistics of the crack area per joints in SAC305 and IND276 after 5800 cycles under TCT -40/125°C.

Both the crack ratio from the cross sections and the statistics of the crack areas after Dye & Pry show IND276 exhibited better crack resistance than SAC305. It had much improved thermal fatigue performance. The data in this work suggested that alloying with 5.5 wt.% of Sb can effectively improve the reliability of solder joints. Presumably, the mechanisms involve solid solution strengthening and precipitation hardening as well as the beneficial effect brought by Sb to slow down the IMC layer growth. To get optimized strengthening, the Sb content was set to 5.5 wt.%, which could provide enough Sb to have both solid solution strengthening and precipitation hardening. With 5.5wt.% of Sb, the alloy may have the optimized volume fraction of micro-sized SnSb intermetallic precipitates which are reported by Lu, et al. [22] and El-Daly, et al. [23] to be distributed throughout the Sn dendrites. In this case, the SbSn precipitates form within the Sn dendrites, unlike the well-known SAC Ag_3Sn mechanism, where the precipitates form at the Sn dendrite boundaries. Presumably, the SbSn precipitates work to resist recrystallization by strengthening the Sn dendrites [24].

CONCLUSIONS

Thermal performance of five Sn/3.2Ag/0.7Cu/xSb (x in range of 4.5 to 6.5 wt.%) alloys were compared to select the optimized Sb content. Based on shear testing at various temperatures and at different intervals of TCT -40 to 125°C, 90.6Sn/3.2Ag/0.7Cu/5.5Sb (IND276) showed the best performance in those Sb-containing alloys. Thus, this composition with the addition of 5.5 wt.% of Sb was identified and developed for testing in targeting high reliability with a wide service temperature capability. IND276 has a melting temperature range from 223–232°C and could be processed with traditional SAC305 reflow profiles. The crack resistance of IND276 in the components of CABGA192 and chip resistors are better than SAC305 under thermal cycling of -40 to 125°C. Alloying with 5.5 wt% of Sb dramatically improved the thermal fatigue resistance compared to SAC305.

REFERENCES

[1] Geng, J., Zhang, H., Mutuku, F. and Lee, N. C., "Sn3.2Ag0.7Cu5.5Sb Solder Alloy with High-Reliability Performance up to 175°C," IPC APEX Expo 2018, 24-25 February 2018, San Diego, Calif.

[2] Geng, J., Zhang, H., Mutuku, F. andLee, N. C., "Novel Solder Alloy: Wide Service Temperature Capability for Automotive Applications," in *IEEE Power Electronics Magazine*, vol. 5, no. 3, pp. 56-62, Sept. 2018.

[3] ChoudhuryP. et al., "New Developments in High Reliability High Temperature Pb Free Alloys". International Conference on Soldering & Reliability (ICSR), Toronto - Canada, May 2014.

[4] R. Raut et al., "Assembly Interconnect Reliability in Solid State Lighting Applications – Part 1". SMTA Pan Pacific Conference, Hawaii, 2011.

[5] Y.H. Ko, S.-H. Yoo, and C.-W. Lee, "Evaluation on Reliability of High Temperature Lead-Free Solder for Automotive Electronics," Journal of the Microelectronics and Packaging Society, Vol. 17, No. 4, pp. 35–40, 2010.
[6] B. Arfaei, F.M. Mutuku, R. Coyle, and E. Cotts, "Influence of Micro-alloying elements on Reliability of SnAgCu Solder Joints", SMTA Journal Vol. 29 Issue 2, 2016.
[7] S. K. Kang, P. Lauro, D. Y. Shih, D. W. Henderson, J. Bartelo, T. Gosselin, and W. K. Choi, (2004). The microstructure, thermal fatigue, and failure analysis of near-ternary eutectic Sn-Ag-Cu solder joints. Materials Transactions, 45(3), 695-702.
[8] J. Zhao, L. Qi, X. M. Wang and L. Wang (2004). "Influence of Bi on microstructures evolution and mechanical properties in Sn–Ag–Cu lead-free solder". Journal of Alloys and Compounds, 375(1), 196-201.
[9] K. N. Reeve, J. R. Holaday, S. M. Choquette, I. E. Anderson, and C. A. Handwerker (2016). "Advances in Pb-free solder microstructure control and interconnect design." Journal of Phase Equilibria and Diffusion, 37(4), 369-386.
[10] A. Z. Miric, (2010). "New developments in high-temperature, high-performance lead-free solder alloys." Balance, 90, 91-6.
[11] C. Handwerker, U. Kattner, and K. W. Moon (2007). "Fundamental properties of Pb-free solder alloys." Lead-Free Soldering, 21-74.
[12] S. K. Kang (2012). "Effects of minor alloying additions on the properties and reliability of Pb-free solders and joints." Lead-free solders: materials reliability for electronics. John Wiley & Sons Ltd, 119-59.
[13] R. Coyle, et al., "The Effect of Bismuth, Antimony, or Indium on the Thermal Fatigue of High Reliability Pb-Free Solder Alloys," Proceedings of SMTAI, Rosemont, IL, October 2018.
[14] R. Coyle, et al., "Enhancing Thermal Fatigue Reliability of Pb-Free Solder Alloys with Additions of Bismuth and Antimony," Proceedings of SMTAI, October 2020.
[15] Max Hansen, Constitution of Binary Alloys, 2nd edition, McGraw-Hill, 1175-1177, 1958.
[16] Rodney P. Elliot, Constitution of Binary Alloys, First Supplement, McGraw-Hill, 802, 1965.
[17] Anton-Zoran Miric, "New Developments in High-Temperature, High-Performance Lead-Free Solder Alloys," SMTA Journal, Volume 23, Issue 4, 24-29, 2010.
[18] W. Liu, N.C. Lee, "High-reliability lead-free solder alloys for harsh environment electronics applications," US Patent 11413709B2, issued August 16, 2022.
[19] Li, G.Y., Chen, B.L., Tey, J.N., "Reaction of Sn-3.5Ag-0.7Cu-xSb solder with Cu metallization during reflow soldering," IEEE Transactions on Electronics Packaging Manufacturing, vol. 27, no. 1, 77-85, 2004.
[20] Li, G.Y., Bi, X.D., Chen, Q., Shi, X.Q., "Influence of dopant on growth of intermetallic layers in Sn-Ag-Cu solder joints," Journal of Electronic Materials, vol. 40, no. 2,165-175, 2011.
[21] Per-Erik Tegehall "Review of the Impact of Intermetallic Layers on the Brittleness of Tin-Lead and Lead-Free Solder Joints, Section 3, Impact of Intermetallic Compounds on the Risk for Brittle Fractures" IVF Project Report 06/07, IVF Industrial Research and Development Corporation, 2006.
[22] S. Lu, Z. Zheng, J. Chen, F. Luo, "Microstructure and solderability of Sn-3.5Ag-0.5Cu-xBi-ySb solders," Proceedings 11th International Conference on Electronic Packaging Technology and High-Density Packaging, ICEPT-HDP 2010, 410-412, 2010.
[23] A.A. El-Daly, Y. Swilem and A.E.Hammad, "Influences of Ag and Au Additions on Structure and Tensile Strength of Sn-5Sb Lead Free Solder Alloy," J. Mater. Sci. Technol., vol.24, no. 6, 921-925, 2008.
[24] G. E. Dieter, Mechanical Metallurgy, Chapter 6, "Dislocation Theory" 159, McGraw-Hill, 1961.